Research on Turbulent Skin Friction Reduction with the aid of Direct Numerical Simulation

Koji Fukagata*

* Department of Mechanical Engineering, Keio University, Hiyoshi 3-14-1, Kohoku-ku, Yokohama 223-8522, Japan
(Tel : +81-45-566-1517; E-mail: fukagata@mech.keio.ac.jp)

Abstract: We introduce a series of studies on turbulent skin friction drag reduction in wall-turbulence. First, an identity equation relating the skin friction drag and the Reynolds shear stress (the FIK identity) is introduced. Based on the implication of the FIK identity, a new analytical suboptimal feedback control law requiring the streamwise wall-shear stress only is introduced and direct numerical simulation (DNS) results of turbulent pipe flow with that control is reported. We also introduce DNS of an anisotropic compliant surface and parameter optimization using an evolutionary optimization technique.

Keywords: Flow control, Wall-turbulence, Theory, Direct numerical simulation.

1. INTRODUCTION

Control of turbulent flows and associated transport phenomena should be a key in many engineering practices such as energy saving, efficient production process, securing high quality products, and resolving global environmental problems; its impacts on future technology and human life would be enormous through manipulation and modification of turbulent drag, noise, heat transfer, mixing as well as chemical reaction[1].

In fiscal years of 2000-2004, a joint research project on turbulence control (Project for Organized Research Combination System by the Ministry of Education, Culture, Sports and Technology of Japan) was conducted in Japan. The project consisted of three different topics, i.e., feedback control using microelectromechanical systems (MEMS), turbulent drag reduction using functionalized fluids (polymer/surfactant/micro-bubble added fluids), and control of combustion, and extensive achievement has been made. In the field of feedback control using MEMS, in addition to the achievement in the theory introduced below, we were able to develop a control system prototype with micro-sensor array, miniature actuators and a controller, as shown in Fig. 1, and achieved 6% drag reduction in a wind-tunnel experiment[2].

In the present paper, we present some of the theoretical achievements in the field of turbulent skin friction reduction made in the above-mentioned project. Also we introduce some related continuation work. The paper is organized as follows. In Section 2, we introduce some mathematical relationships concerning the skin friction reduction control. In Section 3, we introduce an attempt to develop a feedback control law based on the implication of that mathematical relationship. In Section 4, the same idea is applied to a passive control.

2. MATHEMATICAL RELATIONSHIPS CONCERNING SKIN FRICTION REDUCTION CONTROL

2.1 The FIK identity

In wall turbulence, quasi-streamwise vortices (QSVs) are known to play a dominant role in near-wall turbulent transport phenomena[3-5] through their regeneration mechanism[6]. Through an analysis of direct numerical simulation (DNS) data, Kravchenko et al.[7] clearly illustrated that the streamwise vorticity accompanied by QSV strongly correlates with the immediate upstream wall shear stress. Moreover, QSV dominates the production, destruction, and diffusion of the Reynolds shear stress responsible for turbulent friction drag[3].

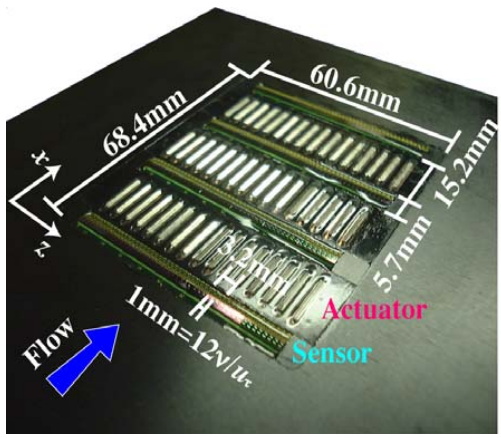

Fig. 1 Feedback control system for wall turbulence with 192 wall shear stress sensors and 48 shell-deformation actuators made by Yoshino et al.[2].

Although it had been known that QSV is responsible for large friction drag in wall turbulence, the quantitative relationship between the turbulent structure and the resultant value of skin friction had not been unknown for a long time. It is a surprise to know that the simple mathematical relationship between the skin friction coefficient and the Reynolds stress distribution (hereafter referred to as the FIK identity) has been derived only recently by Fukagata et al.[8]. In the followings, we briefly review the derivation of that relationship and its implication.

Here, only the simplest case, i.e., a steady, fully-developed, isothermal, incompressible turbulent flow of a Newtonian fluid in a plane channel, as shown in Fig. 2, is considered. The Reynolds averaged Navier-Stokes equation in the streamwise (x) direction is given by

$$0 = -\frac{d\bar{p}}{dx} + \frac{d}{dy}\left[\frac{1}{\mathrm{Re}_b}\frac{d\bar{u}}{dy} + (-\overline{u'v'})\right], \qquad (1)$$

where the overbar denotes the average. In this section, all variables without superscript are those nondimensionalized by the channel half width, δ^*, and twice the bulk mean velocity, $2U_b^*$, whereas dimensional variables are denoted by the superscript of *. The bulk Reynolds number is defined as $\mathrm{Re}_b = 2U_b^*\delta^*/\nu^*$, where ν^* is the kinematic viscosity. The pressure in Eq. (1) is normalized by the density.

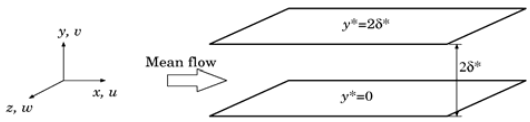

Fig. 2 Flow geometry.

The flow rate is assumed to be always constant. The velocities on the walls are no-slip, but wall-transpiration is allowed given the net flux is zero. This enables the use of the FIK identity to, for instance, a flow controlled by blowing/suction with zero net flux, which is widely used in numerical studies of active feedback control.

Under the conditions above, integration of Eq. (1) over y gives the relation between the pressure gradient and the skin friction coefficient,

$$C_f = \frac{\tau_w^*}{(1/2)\rho^* U_b^{*2}} = \frac{8}{\mathrm{Re}_b}\left.\frac{d\bar{u}}{dy}\right|_{y=0} = -8\frac{d\bar{p}}{dx}. \tag{2}$$

The relation for componential contributions of different dynamical effects to the local skin friction coefficient can be obtained by applying triple integration to Eq. (1). The first integration gives the well-known linear relation for stresses, which is readily derived from Eqs. (1) and (2) as

$$\frac{1}{\mathrm{Re}_b}\frac{d\bar{u}}{dy} + (-\overline{u'v'}) = \frac{C_f}{8}(1-y). \tag{3}$$

The further integration leads to the mean velocity profile, which reads

$$\bar{u} = \mathrm{Re}_b\left[\frac{C_f}{8}\left(y - \frac{y^2}{2}\right) - \int_0^y (-\overline{u'v'})dy\right]. \tag{4}$$

The final integration is akin to obtaining the flow rate from the velocity profile, i.e.,

$$\frac{1}{2} = \mathrm{Re}_b\left[\frac{C_f}{24} - \int_0^1\left\{\int_0^y (-\overline{u'v'})dy\right\}dy\right], \tag{5}$$

where the relation of the dimensionless bulk mean velocity, U_b = 1/2, was used. The double integration in Eq. (5) can be transformed to single integration by applying the integration by parts, viz.,

$$\begin{aligned}\int_0^1\left\{\int_0^y (-\overline{u'v'})dy\right\}dy &= \int_0^1\left\{1\cdot\int_0^y (-\overline{u'v'})dy\right\}dy \\ &= \left[y\int_0^y (-\overline{u'v'})dy\right]_0^1 - \int_0^1 y(-\overline{u'v'})dy \\ &= \int_0^1 (1-y)(-\overline{u'v'})dy.\end{aligned} \tag{6}$$

Thus, Eq. (5) can be rewritten as

$$C_f = \frac{12}{\mathrm{Re}_b} + 12\int_0^1 2(1-y)(-\overline{u'v'})\,dy\,. \tag{7}$$

This identity equation for a fully-developed channel flow indicates that the skin friction coefficient is decomposed into the laminar contribution, $12/\mathrm{Re}_b$, which is identical to the well-known laminar solution, and the turbulent contribution (the second integral term), which is proportional to the weighted average of Reynolds stress. The weight linearly decreases with the distance from the wall.

A similar relationship can be derived also for other canonical flows. The FIK identity for a fully-developed cylindrical pipe flow is expressed as

$$C_f = \frac{16}{\mathrm{Re}_b} + 16\int_0^1 2r\,\overline{u_r' u_z'}\,r dr, \tag{8}$$

where the length is nondimensionalized by the pipe radius. The wall and the cylindrical axis are located at r = 1 and r = 0, respectively.

Note that similar identity equation has been presented also by Bewley and Aamo[9]. Although they presume a laminar base flow in the channel, the final expression is essentially similar to the FIK identity. It is also worth noting that Sbragaglia and Sugiyama[10] extended the FIK identity to general shaped ducts. Their formulation is based on the constant pressure gradient condition instead of constant flow rate, and the resultant expression reads,

$$\langle u\rangle - \langle\tilde{u}\rangle = \langle(\mathbf{uu}):\nabla\tilde{u}\rangle, \tag{9}$$

where the bracket denotes the bulk-average and the tilde indicate the velocity in the Stokes flow under the same pressure gradient.

The FIK identity can be derived for a spatially developing flow. For a zero-pressure-gradient boundary layer on a flat plate it reads

$$\begin{aligned}C_f = \frac{4(1-\delta_d)}{\mathrm{Re}_\delta} &+ 4\int_0^1 (1-y)(-\overline{u'v'})\,dy \\ &- 2\int_0^1 (1-y)^2\left(\frac{\partial\overline{uu}}{\partial x} + \frac{\partial\overline{uv}}{\partial y}\right)dy,\end{aligned} \tag{10}$$

where the nondimensionalization is based on the free-stream velocity and the 99% boundary layer thickness. The third term is the contribution from the spatial development, while δ_d in the first term is the dimensionless displacement thickness. For a laminar plane boundary layer, the first contribution is $4(1\text{-}\delta_d)/\mathrm{Re}_\delta \approx 2.6/\mathrm{Re}_\delta$ and the third contribution can be computed as $2.6/\mathrm{Re}_\delta$ by using the similar solution of Howarth[11]. The summation of these contributions is identical to the well-known relation, i.e., $C_f \approx 3.3/\mathrm{Re}_\delta$.

A more general form of the FIK identity including different dynamical effects (e.g., for channel flows) can be expressed as

$$C_f = \frac{12}{\mathrm{Re}_b} + 12\int_0^1 2(1-y)(-\overline{u'v'})\,dy + \text{(III)} + \text{(IV)} + \text{(V)}. \tag{11}$$

The third term is the contribution from the spatial and temporal development, which reads

$$\begin{aligned}\text{(III)} = 12\int_0^1 (1-y)^2\Bigg(&-\frac{\partial(uu)''}{\partial x} - \frac{\partial(uv)''}{\partial x} \\ &+ \frac{1}{\mathrm{Re}_b}\frac{\partial^2 u''}{\partial x} - \frac{\partial p''}{\partial x} - \frac{\partial u''}{\partial t}\Bigg)dy,\end{aligned} \tag{12}$$

where the double-prime denotes the deviation of mean quantity from the bulk mean quantity, i.e.,

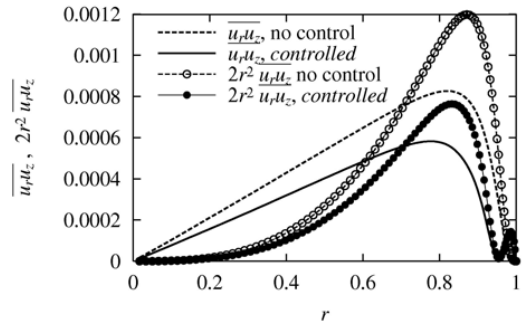

Fig. 3 Reynolds shear stress and weighted Reynolds shear stress in pipe flow at $Re_{\tau 0}$=180 under opposition control[8].

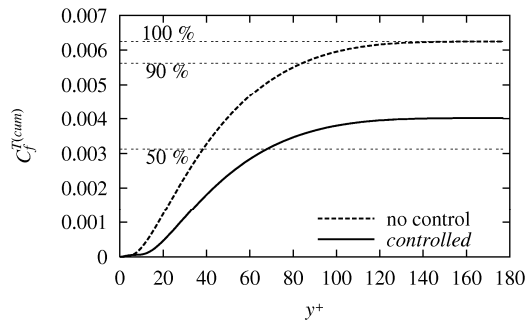

Fig. 4 Cumulative contribution to skin friction in pipe flow at $Re_{\tau 0}$= 180 under opposition control[8].

$$f''(x,y,t) = \overline{f}(x,y,t) - \int_0^1 \overline{f}(x,y,t)\,dy. \tag{13}$$

The fourth term is the contribution from a body force, b_x, and additional stress, τ^a_{xy}, such as that by polymer/surfactant[12-14], which can be expressed as

$$(\mathrm{IV}) = 12\int_0^1 (1-y)\left[(1-y)\overline{b_x} + 2\,\overline{\tau^a_{xy}}\right]dy. \tag{14}$$

The fifth term is the contribution from the boundary momentum flux, such as uniform blowing/suction, which reads

$$(\mathrm{V}) = -12 V_w \int_0^2 (1-y)\overline{u}dy\,, \tag{15}$$

where V_w denotes the wall-normal velocity at the walls. In this case, the integration of the other terms should also be made from 0 to 2, because the flow is not anymore symmetric around the center plane.

2.2 Analysis using the FIK identity

The merit of the FIK identity derived above is that one can quantitatively identify each dynamical contribution to the drag reduction/increase even for a manipulated flow.

The first example is a fully developed turbulent pipe flow manipulated by Choi et al.'s opposition control scheme[15]. Namely, time-dependent, continuous blowing/suction velocity is applied as the boundary condition at the wall, so as to oppose the wall-normal velocity at the detection plane

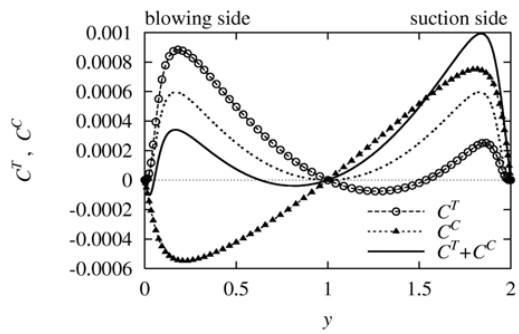

Fig. 5 Contributions to friction drag in channel flow at $Re_{\tau 0}$=150 with uniform blowing and suction[8].

assumed at $y = y_d$. The data were obtained by DNS using the energy-conservative finite difference method[16] at the Reynolds number of Re_b = 5300 (i.e., Re_τ = 180 for uncontrolled flow). The detection plane was set at y_d^+ = 15. Here, the superscript of + denotes a quantity nondimensionalized by the friction velocity of the uncontrolled flow.

Figure 3 shows the Reynolds shear stress, $\overline{u_r' u_z'}$, and the weighted Reynolds shear stress appearing in the FIK identity for pipe flow, i.e., $2r^2\overline{u_r' u_z'}$. As is noticed from Eq. (8), the contribution of Reynolds stress near the wall dominates both in uncontrolled and controlled cases. The difference in the areas covered by these two (controlled and uncontrolled) curves of the weighted Reynolds stress is directly proportional to the drag reduction by control. In the present case, the turbulent contribution is reduced by 35%, while the total drag reduction is 24%. The contribution of Reynolds stress near the wall can be more clearly illustrated by plotting a cumulative contribution, $C_f^{T(cum)}$, to the turbulent part, defined here as

$$C_f^{T(cum)}(y) = 16\int_0^{1-y} 2r\,\overline{u_r' u_z'}\,rdr\,, \tag{16}$$

where $y=(1-r)$ is the distance from the wall. As is shown in Fig. 4, the Reynolds stress within 80 wall units from the wall is responsible for 90% of the turbulent contribution to the skin friction in the case of uncontrolled flow. This fact makes the opposition control algorithm proposed by Choi et al.[15] very successful. Namely, it works to suppress the Reynolds stress near the wall, which results in considerable drag reduction at a low Reynolds number flow. A more interesting analysis can be made when the feedback control is applied only periodically and partially to the wall[17], where the sreamwise variation of C_f can be decomposed into different dynamical contribution through the analysis similar to the budget analysis of Reynolds stress.

Another example of controlled flow is a fully developed channel flow with uniform blowing on one wall and suction on the other. Figure 5 shows the componential contributions computed from the DNS database of Sumitani and Kasagi[18], where the blowing/suction velocity is $V_w = V_w^*/(2U_b^*)$ = 0.00172. The key in the figure, C^T, denotes the integrand of turbulent contribution, and C^C corresponds to that of the convective contribution (see, Eq. (15)). The dotted line in the figure represents C^T in an ordinary channel flow (V_w = 0) at the same bulk Reynolds number (Re_b = 4360), computed by the pseudospectral DNS code[19]. The weighted Reynolds shear stress on the blowing side (defined here, for convenience,

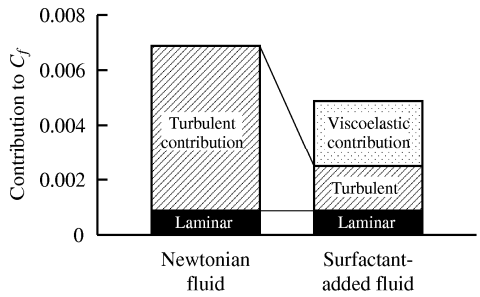

Fig. 6 Contributions to friction drag in surfactant-added channel flow. Redrawn based on Yu et al.[12].

as $0 \le y \le 1$) is larger than that in the case of $V_w = 0$, while it is close to zero on the suction side ($1 \le y \le 2$). The total turbulent contribution is slightly reduced from the ordinary channel flow. The integrand of convective contribution, C^C, is negative on the blowing side and positive on the suction side. The total convective contribution is slightly positive. Since the total convective contribution exceeds the amount of reduction in the turbulent contribution, the total C_f results in a larger value than that of the ordinary channel flow.

The last example is a surfactant-added channel flow performed by Yu et al.[12]. Direct numerical simulation is performed by assuming the Giesekus fluid model. The bulk Reynolds number is 12000. The friction Weisenberg number, which represents the memory effect of the surfactant-added fluid, is 54, corresponding to 75 ppm CTAC surfactant solution. The fractional contribution to C_f is shown in Fig. 6, where the turbulent contribution drastically decreases with the addition of surfactant. The viscoelastic contribution (see, Eq. (14)), however, works to largely increase the friction drag. As a result of these changes, the total friction drag is reduced by about 30%. A similar trend is also reported for experimental data of polymer-added zero-pressure-gradient boundary layer[14]. The changes in the different contributions are found qualitatively similar to the case of the surfactant-added flow mentioned above. Likewise, the FIK identity can be used for investigation of drag reduction mechanism by other additives, such as microbubbles[20].

2.3 The lower bound for net power

The FIK identity further suggests that a drastic drag reduction can be achieved if the near-wall Reynolds shear stress is more ideally reduced. When an ideal feedback body force (instead of blowing/suction) was applied to DNS, the near-wall Reynolds shear stress became negative to yield a friction drag much lower than that of the laminar flow at the same Reynolds number[21].

An essential question with regard to the active control is the lower bound of net power (i.e., pumping plus actuation). For this question, Fukagata et al.[22] have given a mathematical proof very recently. It says that the lowest net power required for driving an incompressible constant mass-flux flow in a periodic duct having arbitrary constant-shape cross-section, when controlled via a distribution of zero-net mass-flux blowing/suction over the no-slip channel walls or via any body forces, is exactly that of the Stokes flow.

2.4 Control effect at practically high Reynolds number

Another question concerning the control targeting at the near-wall turbulent structure is whether the near-wall flow manipulation is still effective even in practical applications at high Reynolds numbers. We theoretically investigated the

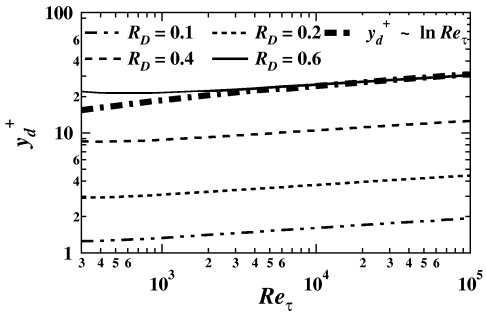

Fig. 7 Thickness of the damping layer, yd, required to achieve the same drag reduction rate, R_D[23].

Reynolds number effect on the drag reduction rate achieved by an idealized near-wall layer manipulation[23]. An assumption is made that all velocity fluctuations in the near-wall layer of $0 < y < y_d$ are perfectly damped. We also assume a fully developed turbulent channel flow under a constant flow rate, and derived a theoretical relationship among the Reynolds number of the uncontrolled flow Re_τ, the dimensionless damping layer thickness y_d/δ, and the drag reduction rate R_D. It is given as

$$\frac{1}{\kappa}\ln \mathrm{Re}_\tau + F = \frac{y_d}{\delta}\left(1 - \frac{y_d}{\delta} + \frac{1}{3}\frac{y_d^2}{\delta^2}\right)(1-R_D)\,\mathrm{Re}_\tau + \left(1-\frac{y_d}{\delta}\right)^{\frac{3}{2}}(1-R_D)^{\frac{1}{2}} \times \left[\frac{1}{\kappa}\ln\left\{\left(1-\frac{y_d}{\delta}\right)^{\frac{3}{2}}(1-R_D)^{\frac{1}{2}}\,\mathrm{Re}_\tau\right\} + F\right]. \quad (17)$$

The sole empirical formula used in the derivation above is the Dean's formula[24] on the bulk mean velocity (the logarithmic law version).

The Reynolds number dependency of y_d required to achieve the same drag reduction rate R_D is shown in Fig. 7. As Re_τ increases, y_d gradually increases. For high Reynolds numbers, where $y_d/\delta << 1$ holds, Eq. (17) can reduce to $y_d^+ \sim \ln Re_\tau$, and this means the Reynolds number dependency is very weak. The asymptotic relation is in good agreement with Eq. (17) when $Re_\tau > 4 \times 10^3$, as shown in Fig. 7. Thus, large drag reduction can be obtained even at high Reynolds numbers if we can control and completely damp the near-wall velocity fluctuations.

Figure 8 shows the flow field computed in the corresponding DNS. The friction Reynolds number is about 650 and the damped layer thickness is $y_d^+ = 60$. The turbulence is drastically suppressed in the damped layer, and found considerably suppressed also in the undamped region. The change in the Reynolds shear stress gives a clue to explain the large drag reduction through the FIK identity. The drag reduction rate directly caused by the decrease of the Reynolds shear stress in the damped layer is 18%, while that due to the accompanied decrease of the Reynolds shear stress in the undamped region is 56%. For higher Reynolds numbers, the relative thickness of the damping layer y_d/δ becomes negligibly small, so that the contribution away from he damped layers should be dominant. Thus, possible large drag reduction at high Reynolds numbers should be mainly attributed to the decrease of the Reynolds stress in the region away from the wall.

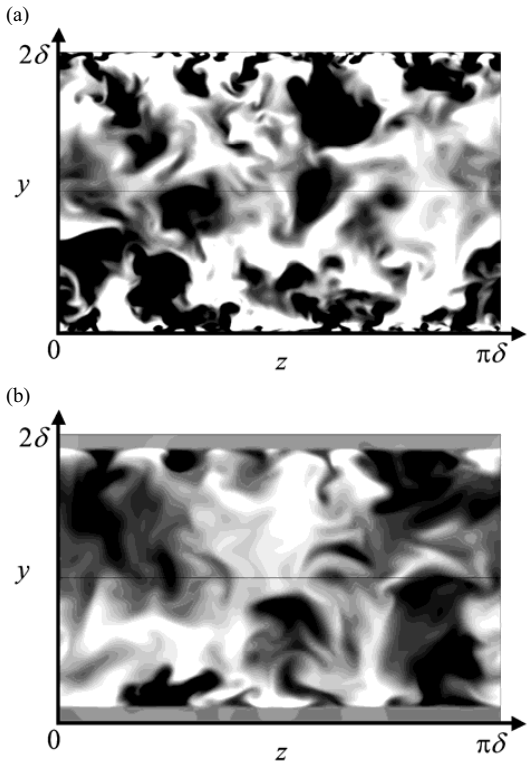

Fig. 8 Cross-sectional view of an instantaneous streamwise velocity in channel flow at Re_τ = 650: (a) uncontrolled; (b) with damping in the near-wall layer[23].

The present theoretical analysis provides a favorable support for the existing control schemes. Namely, attenuation of turbulence in the near-wall layer is still effective at higher Reynolds numbers appearing in real applications.

3. DEVELOPMENT OF NEW ACTIVE CONTROL

3.1 New analytical suboptimal control law

The FIK identity suggests that suppression of the Reynolds shear stress in the near-wall region is of primary importance in order to substantially reduce the skin friction drag. Once the near-wall Reynolds shear stress is suppressed, the stress far from the wall is also suppressed through the indirect effect as shown above. From this argument, a new suboptimal control law was derived by Fukagata and Kasagi[25]. In that work, the cost functional for a channel flow was defined as follows:

$$J(\phi)=\frac{\ell}{2A\Delta t}\int_t^{t+\Delta t}\int_S \phi^2 dSdt+\frac{1}{2A\Delta t}\int_t^{t+\Delta t}\int_S (-u'v')_{y=Y}\,dSdt. \qquad (18)$$

Here, ϕ denotes the local blowing/suction velocity at the wall, A is the area of wall S, △t is the time-span for optimization, and ℓ is the price for the control.

By approximating the Reynolds shear stress at $y = Y$ using the first-order Taylor expansion, viz.,

$$(-u'v')_{y=Y}=-Y\phi\left.\frac{\partial u}{\partial y}\right|_w, \qquad (19)$$

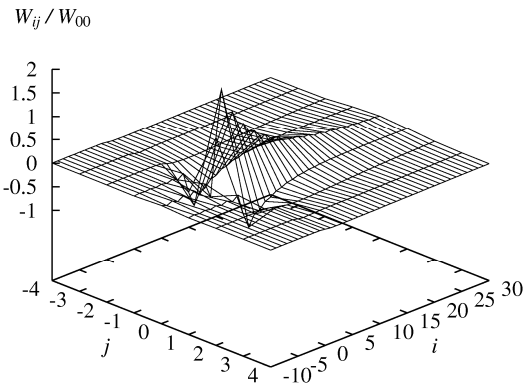

Fig. 9 Weight distributions of the Reynolds shear stress-based suboptimal control law[25].

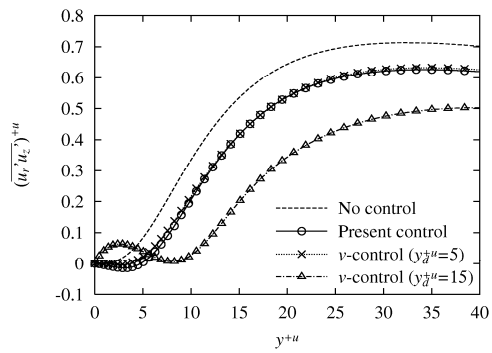

Fig. 10 Reynolds shear stress in pipe flow at Re = 180 under the Reynolds shear stress-based suboptimal control[25].

the control input, ϕ, that minimizes the cost functional can be calculated analytically by the procedure proposed by Lee et al.[26]. The result is

$$\hat{\phi}=\frac{\alpha}{1-i\alpha\gamma k_x/k}\left.\frac{\widehat{\partial u}}{\partial y}\right|_w, \qquad (20)$$

where the hat denotes the Fourier component, $i=\sqrt{-1}$ and $k=\sqrt{k_x^2+k_z^2}$. There are two parameter: $\alpha = Y/(2\ell)$ is the amplitude coefficient and can be interpreted as an inverse of influential length (see, Ref.[26], for details).

A similar control law can be developed also for a pipe flow. Following the procedure by Xu et al.[27], an approximate control law is derived as

$$\hat{\phi}=\frac{\alpha}{1-i\alpha\gamma I_m(k_z)/I_m'(k_z)}\left.\frac{\widehat{\partial u_z}}{\partial r}\right|_w, \qquad (21)$$

where I_m is an mth-order modified Bessel function of the first kind and I'm is its derivative. Although the expressions look different, the control laws for channel and pipe have essentially the same dynamical effect on the controlled flow[25].

The derived control law can be transformed to the physical space through the following inverse Fourier transform, similarly to Lee et al.[26], to read

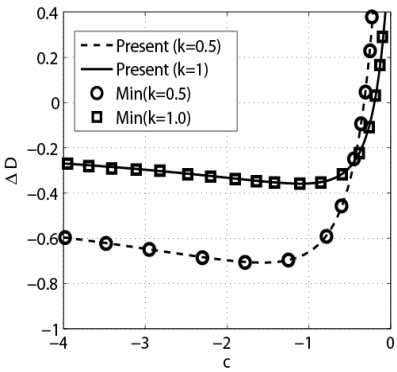

Fig. 11 Drag increment D as functions of wavespeed c and wavenumber k in of Min et al.'s traveling wave control[29] reproduced by Mamori et al.[30].

$$\phi(x,z,t) = \sum_i \sum_j W_{ij} \left.\frac{\partial u}{\partial y}\right|_w (x + i\Delta x,\ z + j\Delta z,\ t), \tag{22}$$

where Δx and Δz are the streamwise and spanwise grid spacings, respectively. The weight distribution in the physical space is shown in Fig. 9. The weights are symmetric in the spanwise direction and asymmetric in the streamwise direction. The product of parameters, $\alpha\gamma$, determines the tail length in the streamwise direction.

Performance of the proposed control algorithm was tested by DNS of turbulent pipe flow[25]. About 12 % drag reduction is obtained when $\phi_{rms}^{+} \approx 0.1$ and $\alpha\gamma = 73$. The profile of the Reynolds shear stress is shown in Fig. 10. As expected, the near-wall Reynolds stress is suppressed by the present control. Note that, the profile of the present control is nearly the same as that of the opposition control (denoted as v-control) with $y_d^{+} = 5$. Comparison is also made with the opposition control with $y_d^{+} = 15$, in which the Reynolds stress around $5 < y^{+} < 10$ is suppressed to give a higher drag reduction rate of 25%. The direct suppression with the present control seems to occur merely in the region of $0 < y^{+} < 5$. This is due to the first-order Taylor expansion used for the approximation of cost functional, i.e., Eq. (19). If the streamwise velocity above the wall, say at $y^{+} = 15$, can be more accurately estimated, a higher drag reduction can be made by this control strategy. In fact, in DNS using the streamwise velocity above the wall as an idealized sensor signal, a drag reduction rate was about 25%[28], which is comparable to the opposition control.

3.2 Traveling wave control by Min et al.[29]

Based in the implication of the FIK identity, Min et al.[29] proposed a novel active predetermined control technique. They applied a traveling wave-like blowing and suction to channel flows. Through the linear analysis of Poiseuille flow and DNS of turbulent channel flow, they found that the upstream traveling wave ($c < 0$ in Fig. 11)can create a large negative Reynolds shear stress and thereby the friction drag can be sustained at a level below that of the laminar flow (i.e., $\Delta D < 0$ in Fig. 11).

It is worth noting that, according to the theorem on the net power[22] introduced above, the net power should be larger than the laminar pumping power even in the case of so-called sublaminar drag. In fact, Hoepffner and Fukagata[31] revisited Min et al.'s control and verified this argument on the total power.

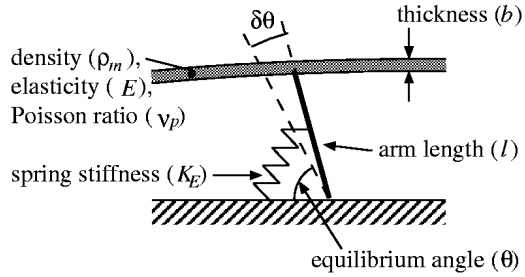

Fig. 12 Anisotropic compliant surface model[32, 33].

4. PASSIVE CONTROL USING ANISOTROPIC COMPLIANT SURFACE

The implication of FIK identity has also been applied to consider a passive control[32]. We consider here a passive control using an anisotropic compliant surface model[33], as illustrated in Fig. 12. Due to the restriction of the inclined arms, this anisotropic compliant surface always moves so as to create a negative Reynolds shear stress on the wall. The membrane equation of motion can be written as

$$b\rho_m \frac{\partial^2 \eta_f}{\partial t^2} + \underbrace{D\frac{\partial \eta_f}{\partial t}}_{\text{damping}} + \underbrace{B\cos^2\theta \nabla^2\nabla^2\eta_f}_{\text{bending of membrane}} - \underbrace{Eb\nabla^2\eta_f}_{\text{tension of membrane}} + \underbrace{K_E\eta_f}_{\text{spring}} = \underbrace{(-p_w' + \sigma_w')\cos\theta}_{\text{pressure + normal stress}} + \underbrace{\tau_w' \sin\theta}_{\text{wall shear stress}}. \tag{23}$$

Here, $\eta_f = l\delta\theta$ is the single variable determining the motion of membrane, and all the symbols are explained in Fig. 12 except for the damper coefficient D and the bending moment B.

We consider an incompressible turbulent channel flow. The fluid velocity field is simulated by using the second-order finite difference code, which was originally developed for pipe flows[16] and later adapted to channel flows[34]. The flow rate is kept constant. The bulk Reynolds number, Re_b, is 3300, which corresponds to a friction Reynolds number of about Re_τ = 113 in the case of rigid walls. The computational domain is $3\delta \times 2\delta \times 3\delta$ and the number of cells is $32 \times 64 \times 64$ in the streamwise (x), the wall-normal (y), and the spanwise (z) directions, respectively. This domain size is similar to that used in the previous study of isotropic compliant surfaces by Xu et al.[35].

The membrane equation of motion is spatially discretized by the second-order accurate finite difference method on the same mesh as that for the wall boundary of the fluid velocity field. The time integration is done by RK3/CN method with the same time stepping as that for the fluid. The membrane is driven by the pressure and wall-shear fluctuations, whereas the velocity of the membrane computed at every instant is used as the boundary condition of the fluid velocity field at the wall.
In order to enable an optimization study, deformation of the membrane is neglected. This simplification is justified when the wall displacement is relatively small (say, less than about 5 wall unit). Note that Kang and Choi[36] from their DNS of feedback-controlled channel flow reported that, when the wall displacement is less than 5 wall unit, the most of the drag reduction is due to the velocity induced by the wall motion rather than the wall displacement. The computational time step is chosen so that both the CFL number for the fluid and that for the membrane are less than 0.5.

(a)

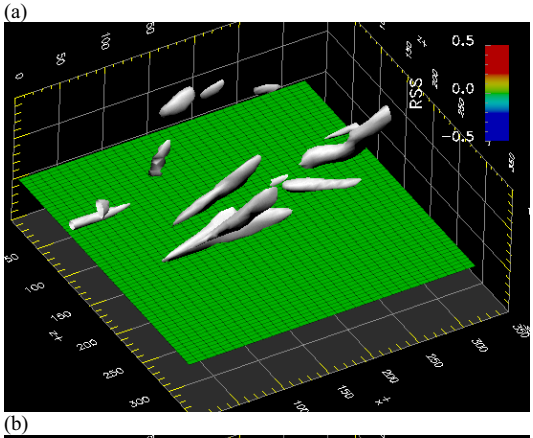

(b)

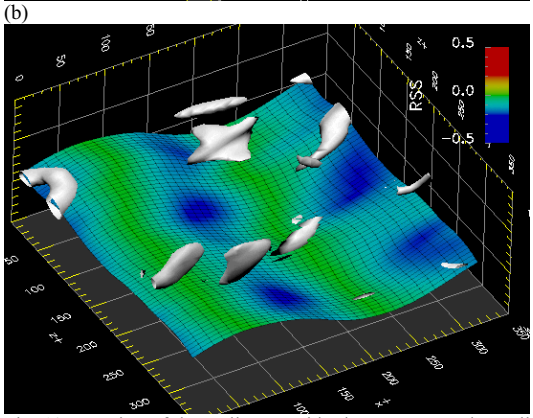

Fig. 13 Motion of the wall, Reynolds shear stress on the wall (color), and the vortical structure (white): (a) solid wall (b) anisotropic compliant surface[32].

The surface model has several parameters that have to be determined. The inverse design problem is formulated as an optimization problem. Our objective is to minimize the friction drag coefficient C_f, which is a function of wall parameters $\boldsymbol{\alpha} = (b, \rho_m, E, K_E, \theta, D)$, under the restriction of wall-deformation amplitude. Therefore, the cost function can be defined here as the friction drag that we want to minimize. We also added a penalty term in order to avoid solutions lading to large deformation.

We implement an Evolution Strategy with Adaptation of the Covariance Matrix (CMA-ES)[37]. The competitive performance and robustness of CMA-ES have been demonstrated in a number of benchmark optimization problems[38] and applications. Based on a preliminary parameter study, we choose a logarithmic encoding for all parameters except θ.

The CMA-ES was initialized with sets of parameters distributed over the initial search domain. The available computation time permitted about 1000 evaluation trials (to be exact, 992 evaluations) of the cost function, each one involving two simulations with different initial turbulent fields (viz., about 2000 DNS runs were made in total).

Figure 13 shows the wall motion of the most drag reducing case (R_D = 8%). The surface deforms in a wavelike manner, which travels in the downstream direction. The wavelength about 330 wall unit (i.e., the same length as the computational domain) and the wavespeed is observed to be $c^{+0} = 4$. In terms of the bulk velocity, this corresponds to $c/U_b = 0.3$.

The Reynolds shear stress on the wall is made largely negative in front of and behind the hill where the wall-velocity is large. The quasi-streamwise vortices observed on the solid wall (Fig. 13(a)) are less populated on the compliant wall (Fig. 13(b)), and instead, spanwise vortical structures are found to be increased. Such spanwise vortices have been observed also in other drag reducing flows under feedback control[21, 39]. Although its generation mechanism and its role in drag reduction are not fully clear, it is conjectured that they work as "rollers" between the wall and the bulk flow[39].

5. SUMMARY

In the present paper, we have introduced the identity equation between the Reynolds shear stress and the skin friction (the FIK identity) and some example of DNS of turbulent pipe and channel flows for skin friction reduction based on the implication of the identity equation. DNS is a powerful tool for flow control study and, of course, it can be applied for other types of flow. For instance, in the author's group, an active control of mixing layer by means of flapping actuator[40] and a passive control of flow around a cylinder by using porous media[41] are currently studied by means of DNS. Interested readers are referred to the papers cited above.

ACKNOWLEDGMENTS

The author thanks his co-workers, especially, Drs. N. Kasagi, Y. Suzuki, K. Sugiyama (The University of Tokyo), K. Iwamoto (Tokyo University of Agriculture and Technology), S. Obi (Keio Univiersity), J. Hoepffner (Pierre and Marie Curie University), Messers. Y. Naka, H. Mamori, H. Naito, K. Shimada, and Y. Kametani (Keio University). The author also acknowledges Korean Society of Computational Fluid Engineering (KSCFE) and Japan Society of Fluid Mechanics (JSFM) for the invitation to this workshop. Large part of the work introduced here was conducted through Project for Organized Research Combination System by the Ministry of Education, Culture, Sports and Technology (MEXT) of Japan.

REFERENCES

[1] 2009, Kasagi, N., Suzuki, Y. and Fukagata, K., "Microelectricalmechanical systems-based feedback control of turbulence for skin friction reduction," *Annu. Rev. Fluid Mech.*, Vol.41, pp.231-251.

[2] 2008, Yoshino, T., Suzuki Y. and Kasagi, N., "Feedback control of turbulence air channel flow with distributed micro sensors and actuators," *J. Fluid Sci. Tech.*, Vol.3, pp.137-148.

[3] 1995, Kasagi, N., Sumitani, Y., Suzuki, Y. and Iida, O., "Kinematics of the quasi-coherent vortical structure in near-wall turbulence," *Int. J. Heat Fluid Flow* Vol.16, pp. 2-10.

[4] 1967, Kline, S.J., Reynolds, W.C., Schraub, F. A. and Runstadler, P. W., "The structure of turbulent boundary layers," *J. Fluid Mech.*, Vol.30, pp.741-773.

[5] 1991, Robinson, S.K. "Coherent motions in the turbulent boundary layer," *Annu. Rev. Fluid Mech.*, Vol. 23, pp.601-639.

[6] 1995, Hamilton, J.M., Kim, J. and Waleffe, F., "Regeneration mechanisms of near-wall turbulence structures, " *J. Fluid Mech.*, Vol.287, pp.317-348.

[7] 1993, Kravchenko, A.G., Choi, H. and Moin, P., "On the relation of near-wall streamwise vortices to wall skin friction in turbulent boundary layers," *Phys. Fluids A*, Vol.5, pp.3307-3309.

[8] 2002, Fukagata, K., Iwamoto, K. and Kasagi, N.,

"Contribution of Reynolds stress distribution to the skin friction in wall-bounded flows," *Phys. Fluids*, Vol.14, L73-L76.

[9] 2004, Bewley, T.R. and Aamo, O.M., "A ``win-win" mechanism for low-drag transients in controlled 2D channel flow and its implications for sustained drag reduction," *J. Fluid Mech.*, Vol.499, pp.183-196.

[10] 2007, Sbragaglia, M. and Sugiyama, K., "Boundary induced nonlinearities at small Reynolds numbers," *Physica D*, Vol.228, pp.140-147.

[11] 1938, Howarth, L., "On the solution of the laminar boundary layer equations," *Proc. Roy. Soc. London Ser. A*, Vol.164, pp.547-579.

[12] 2004, Yu, B., Li, F. and Kawaguchi, Y., "Numerical and experimental investigation of turbulent characteristics in a drag-reducing flow with surfactant additives," *Int. J. Heat Fluid Flow*, Vol.25, pp.961-974.

[13] 2004 Li, F.-C., Kawaguchi, Y. and Hishida, K. 2004 "Investigation on the characteristics and turbulent transport for momentum and heat in a drag-reducing surfactant solution flow," *Phys. Fluids*, Vol.16, pp. 3281-3295.

[14] 2006, Hou, Y., Sommandepalli, V.S.R. and Mungal, M.G., "A technique to determine total shear stress and polymer stress profiles in drag reduced boundary layer flows,", *Exp. Fluids*, Vol.40, pp.589-600.

[15] 1994, Choi, H., Moin, P. and Kim, J., "Active turbulence control for drag reduction in wall-bounded flows," *J. Fluid Mech.*, Vol.262, pp.75-110.

[16] 2002, Fukagata, K. and Kasagi, N., "Highly energy-conservative finite difference method for the cylindrical coordinate system," *J. Comput. Phys.*, Vol. 181, pp.478-498.

[17] 2003, Fukagata, K. and Kasagi, N., "Drag reduction in turbulent pipe flow with feedback control applied partially to wall," *Int. J. Heat Fluid Flow*, Vol.24, pp. 480-490.

[18] 1995, Sumitani, Y. and Kasagi, N., "Direct numerical simulationof turbulent transport with uniform wall injection and suction," *AIAA J.*, Vol.33, pp.1220-1228.

[19] 2002, Iwamoto, K., Suzuki, Y. and Kasagi, N. "Reynolds number effect on wall turbulence: toward effective feedback control," *Int. J. Heat Fluid Flow*, Vol. 23, pp.678-689.

[20] 2007, Xu, J., Dong, S., Maxey, M. and Karniadakis, G., "Turbulent drag reduction by constant near-wall f orcing," *J. Fluid Mech.*, Vol.582, pp.79-101.

[21] 2005, Fukagata, K., Kasagi, N. and Sugiyama, K., "Feedback control achieving sublaminar friction drag," *Proc. 6th Symp. Smart Control of Turbulence, Tokyo, March 2005*, pp.143-148.

[22] 2008, Fukagata, K., Sugiyama, K. and Kasagi, N., "On the lower bound of net driving power in controlled duct flows," *Physica D*, submitted.

[23] 2005, Iwamoto K., Fukagata, K., Kasagi, N. and Suzuki Y., "Friction drag reduction achievable by near-wall turbulence manipulation at high Reynolds number," *Phys. Fluids*, Vol.17, Art. No. 011702.

[24] 1978, Dean R. B., "Reynolds number dependence of skin friction and other bulk flow variables in two-dimensional rectangular duct flow," *Trans. ASME J. Fluids Eng.*, Vol.100, pp.215-223.

[25] 2004, Fukagata, K. and Kasagi, N., "Suboptimal control for drag reduction via suppression of near-wall Reynolds shear stress," Int. J. Heat Fluid Flow, Vol.25, pp. 341-350.

[26] 1998, Lee, C., Kim, J. and Choi, H., "Suboptimal control of turbulent channel flow for drag reduction," *J. Fluid Mech.*, Vol.358, pp.245-258.

[27] 2002, Xu, C.-X., Choi, J.-I. and Sung H. J., "Suboptimal control for drag reduction in turbulent pipe flow," *Fluid Dyn. Res.*, Vol.30, pp.217-231.

[28] 2004, Fukagata, K. and Kasagi, N., "Feedback control of near-wall Reynolds shear stress in wall-turbulence," *Proc. 4th Int. Symp. Advanced Fluid Information and Transdisciplinary Fluid Integration, Sendai, Nov. 2004*, pp.346-351.

[29] 2006, Min, T., Kang, S.M., Speyer, J.L. and Kim, J., "Sustained sub-laminar drag in a fully developed channel flow," *J. Fluid Mech.*, Vol.558, pp.309-318.

[30] 2008, Mamori, H., Fukagata, K., Hoepffner, J. and Obi, S., "Linear analysis of drag reduction in channel flow by wall heating/cooling," *Proc. 7th EUROMECH Fluid Mech. Conf., Manchester, UK, September 14-18, 2008*, p.207.

[31] 2008, Hoepffner, J. and Fuakgata, K., "Pumping or drag reduction?" *J. Fluid Mech.*, submitted.

[32] 2008, Fukagata, K., Kern, S., Chatelain, P., Koumoutsakos, P. and Kasagi, N., "Evolutionary optimization of an anisotropic compliant surface for turbulent friction drag reduction," *J. Turbulence*, to appear.

[33] 1990, Carpenter, P. W. and Morris, P. J., "The effect of anisotropic wall compliance on boundary-layer stability and transition," *J. Fluid Mech.*, Vol.218, pp.171-223.

[34] 2006, Fukagata, K., Kasagi, N. and Koumoutsakos, P., "A theoretical prediction of friction drag reduction in turbulent flow by superhydrophobic surfaces," *Phys. Fluids*, Vol.18, Art. No. 051703.

[35] 2003, Xu, S., Rempfer, D. and Lumley, J., "Turbulence over a compliant surface: numerical simulation and analysis," *J. Fluid Mech.*, Vol.478, pp.11-34.

[36] 2000, Kang, S. and Choi, H., "Active wall motions for skin-friction drag reduction," *Phys. Fluids*, Vol.12, pp. 3301-3304.

[37] 2001, Hansen, N. and Ostermeier, A., "Completely derandomized selfadaptation in evolution strategies," *EVol.Comput.*, Vol.9, pp.159-195.

[38] 2004, Kern, S., Müller, S.D., Hansen, N., Büche, D., Ocenasek, J. and Koumoutsakos, P., "Learning probability distributions in continuous evolutionary algorithms - a comparative review," *Natural Computing*, Vol.3, pp.77-112.

[39] 1999, Koumoutsakos, P., "Vorticity flux control in a turbulent channel flow," *Phys. Fluids*, Vol.11, pp. 248-250.

[40] 2008, Shimada, K. Fukagata, K. and Obi, S., "Numerical simulation of a plane mixing layer with periodic excitation," *Proc. 7th JSME-KSME Thermal and Fluids Engineering Conf., Sapporo, October 13-16, 2008*, Paper No. 195, No.4..

[41] 2008, Naito, H., Fukagata, K. and Obi, S., "Passive control of flow around a circular cylinder using porous media," *Proc. 7th JSME-KSME Thermal and Fluids Engineering Conf., Sapporo, October 13-16, 2008*, Paper No. 196, No,4.